Electronic Supplementary Information

Experimental section

Materials: Tannic acid (TA), silver nitrate ($AgNO_3$) and K_2CO_3 were purchased from Aladdin Ltd. (Shanghai, China). All reagents were used as received without further purification. The water used throughout all experiments was purified through a Millipore system.

Synthesis of Ag nanosheet: Firstly, 60 mL of 3 mM TA aqueous solution was prepared and taken into the beaker. This solution was adjusted at pH=7 by adding 0.5 M K_2CO_3 aqueous solution. Secondly, 60 mL of 3 mM $AgNO_3$ was added into the above solution with vigorous magnetic stirring for 5 h at room temperature and kept absent of light by using aluminum foil. Thirdly, the reaction mixture was centrifuged at 5000 rpm for 30 min.[1] The obtained precipitate was carefully washed with distilled water and ethanol for a dozen times, aiming to completely remove the NO_3^-. Then, the precipitate was dried at 60 ^{o}C for 12 h. Finally, the dried precipitate was well grinded to obtain the fine powder.

Characterization: XRD data were collected on X-ray diffractometer (Philip Company, Pw1730) equipped with a Cu Kα radiation (λ=1.5418 Å). TEM measurements were carried out on a Zeiss Libra 200FE transmission electron microscope operated at 200 kV. UV-Vis spectra were measured applying a SHIMADZU UV-2700 ultraviolet-visible (UV-Vis) spectrophotometer.

Electrochemical measurement: NRR tests were performed in a two-compartment cell separated by Nafion 211 membrane under ambient condition. The membrane was protonated by first boiling in ultrapure water for 1 h and treating in H_2O_2 (5 wt%) aqueous solution at 80 °C for another 1 h. Then, the membrane was treaded in 0.5 M H_2SO_4 for 3 h at 80 °C and finally in water for 6 h. The electrochemical experiments were tested with an electrochemical workstation (CHI 660E) using a three-electrode configuration with prepared electrode, graphite rod and Ag/AgCl electrode (saturated KCl electrolyte) as working electrode, counter electrode and reference electrode, respectively. The potentials reported in this work were converted to reversible hydrogen electrode (RHE) scale via calibration with the following equation: E (vs. RHE) = E (vs. Ag/AgCl) + 0.256 V and the presented current density was normalized to the geometric surface area. For electrochemical NRR tests, the 0.1 M HCl electrolyte was bubbled with N_2 for 30 min before the measurement.

Determination of NH_3: The concentration of produced NH_3 was spectrophotometrically determined by the indophenol blue method.[2] In detail, 2 mL of post-tested electrolyte was taken from the cathodic compartment and transferred into a 10 mL plastic tube. Then, 2 mL of 1 M NaOH solution (containing 5% salicylic acid and 5% sodium citrate), 1 mL of 0.05 M NaClO and 0.2 mL of 1% $C_5FeN_6Na_2O\cdot 2H_2O$ were added into the above solution. After standing at room temperature and keeping out of the light for 2 h, the UV-Vis absorption was measured at a wavelength of 655 nm. The concentration-absorbance curves were calibrated using standard NH_4Cl solution with a serious of concentrations. The fitting curve ($y = 0.3563x + 0.0427$, $R^2 = 0.999$) shows good linear relation of absorbance value with NH_4^+ concentration by three times independent calibrations. The NH_3 concentration was calculated from the calibration curve and the NH_3 yield rate was calculated using the following equation:

$$NH_3 \text{ yield rate} = (c_{NH3} \times V) / (17 \times t \times A)$$

Where c_{NH3} is the measured NH_3 concentration, V is the volume of electrolyte, t is the reduction reaction time, and A is the geometric area of the cathode (1×1 cm^{-2}).

Determination of FE: Assuming three electrons were needed to produce one NH_3 molecule, the FE in 0.1 M HCl could be calculated as follows:

$$FE = 3F \times c_{NH3} \times V / 17 \times Q$$

Where F is the Faraday constant, Q is the quantity of applied electricity.

Determination of N_2H_4: N_2H_4 presented in the electrolyte was estimated by the method of Watt and Chrisp.[3] A mixed solution of 5.99 g $C_9H_{11}NO$, 30 mL HCl and 300 mL ethanol was used as a color reagent. The calibration curve was plotted as follow: a series of reference solutions with increasing concentration of $N_2H_4\cdot H_2O$ solution were prepared, their calibration concentrations are: 0, 0.1, 0.2, 0.3, 0.4 and

0.5 μg mL^{-1}, and then 5 mL color reagent was added into each solution under stirring for 15 min at room temperature, finally the absorbance was measured at 455 nm. The obtained calibration curve is y=1.0334x + 0.0348, R^2=0.999. The yields of N_2H_4 after NRR electrolysis were estimated by using 5 mL residual electrolyte mixed with 5 mL color reagent (also under stirring for 15 min at 25 ^{o}C).

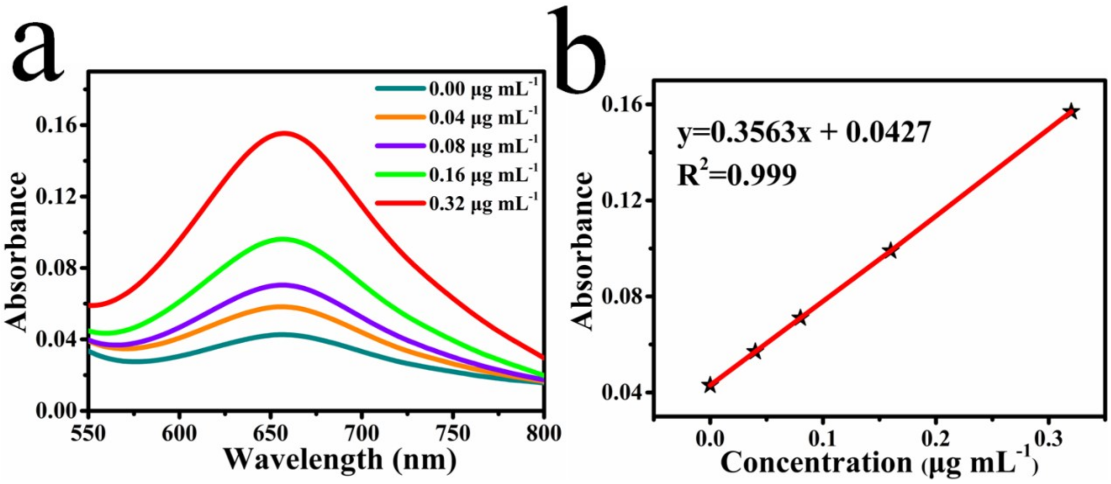

Fig. S1. (a) UV-Vis absorption spectra of indophenol assays with NH_4^+ ions after incubation for 2 h at room temperature. (b) Calibration curve used for estimation of NH_3 concentration.

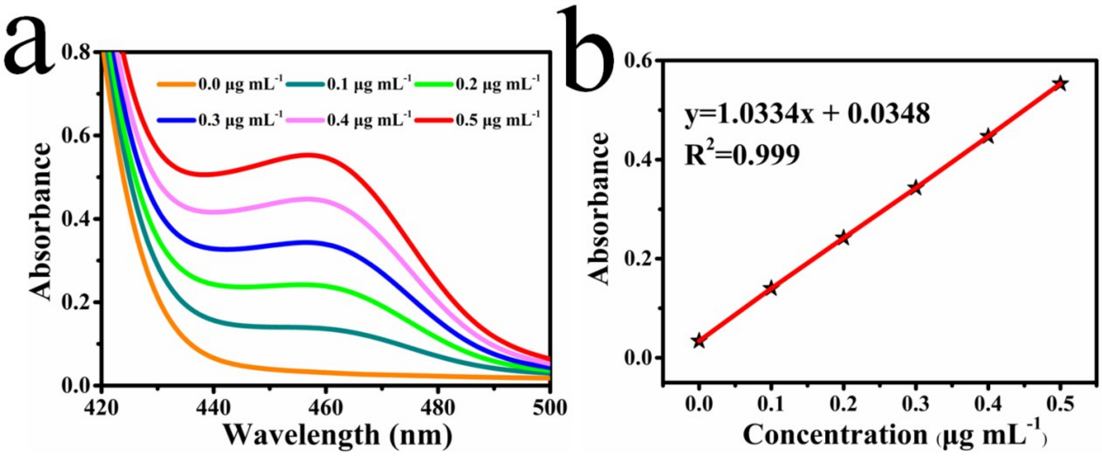

Fig. S2. (a) UV-Vis absorption spectra of various N_2H_4 concentrations after incubation for 15 min at room temperature. (b) Calibration curve used for calculation of N_2H_4 concentrations.

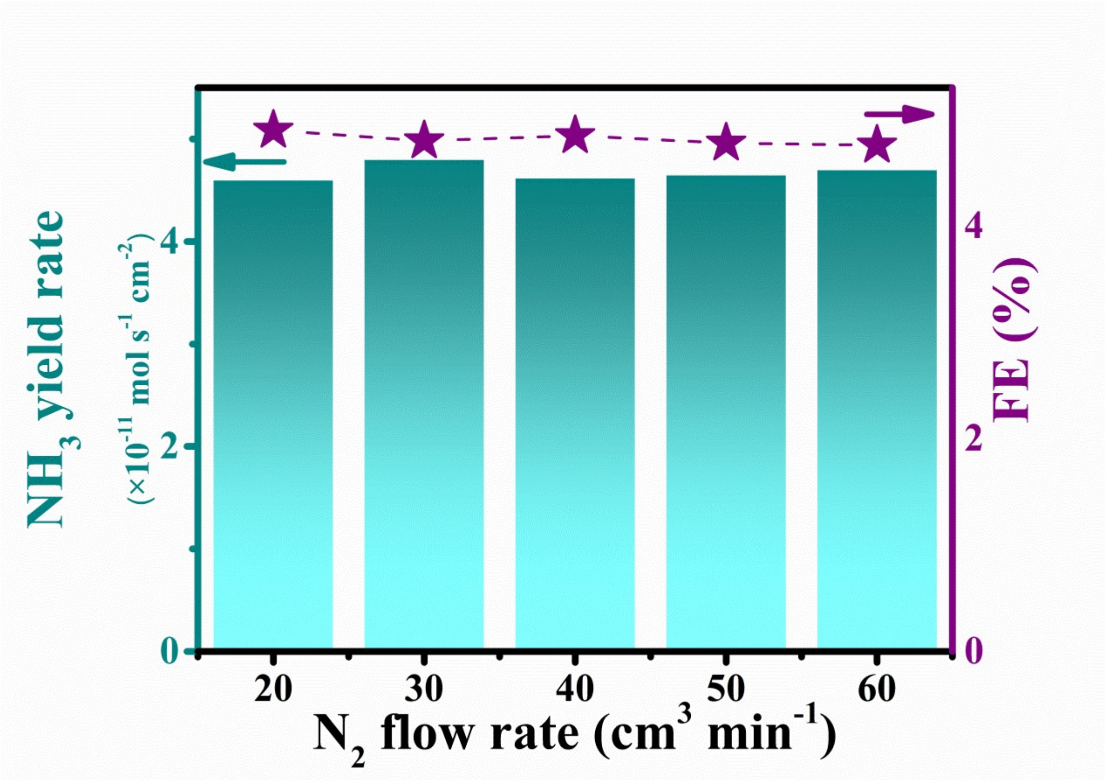

Fig. S3. NH_3 yield rates and FEs of Ag/CPE under different flow rates operated at -0.60 V.

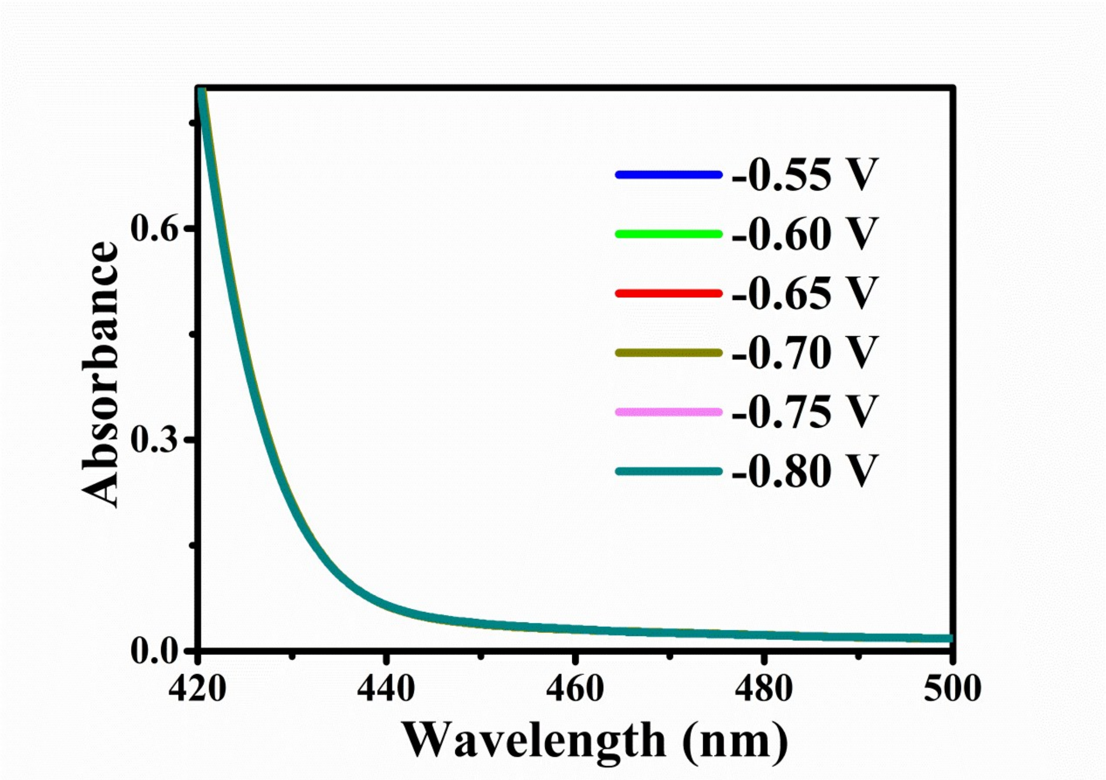

Fig. S4. UV-Vis absorption spectra of electrolytes at each given potential stained with p-$C_9H_{11}NO$ indicator after 2h NRR electrolysis.

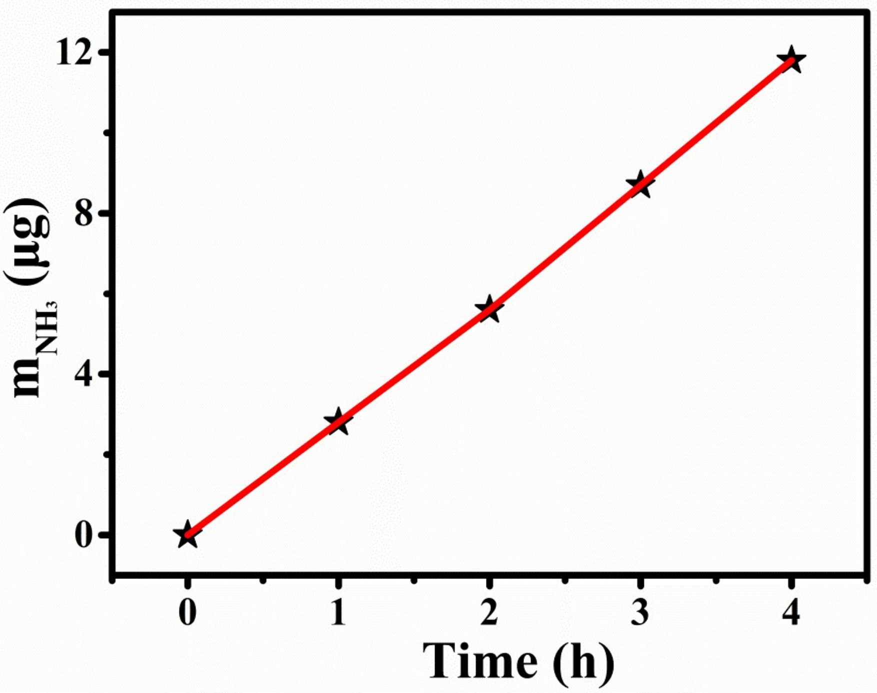

Fig. S5. The amount of NH_3 produced vs. reaction time at -0.60 V

.

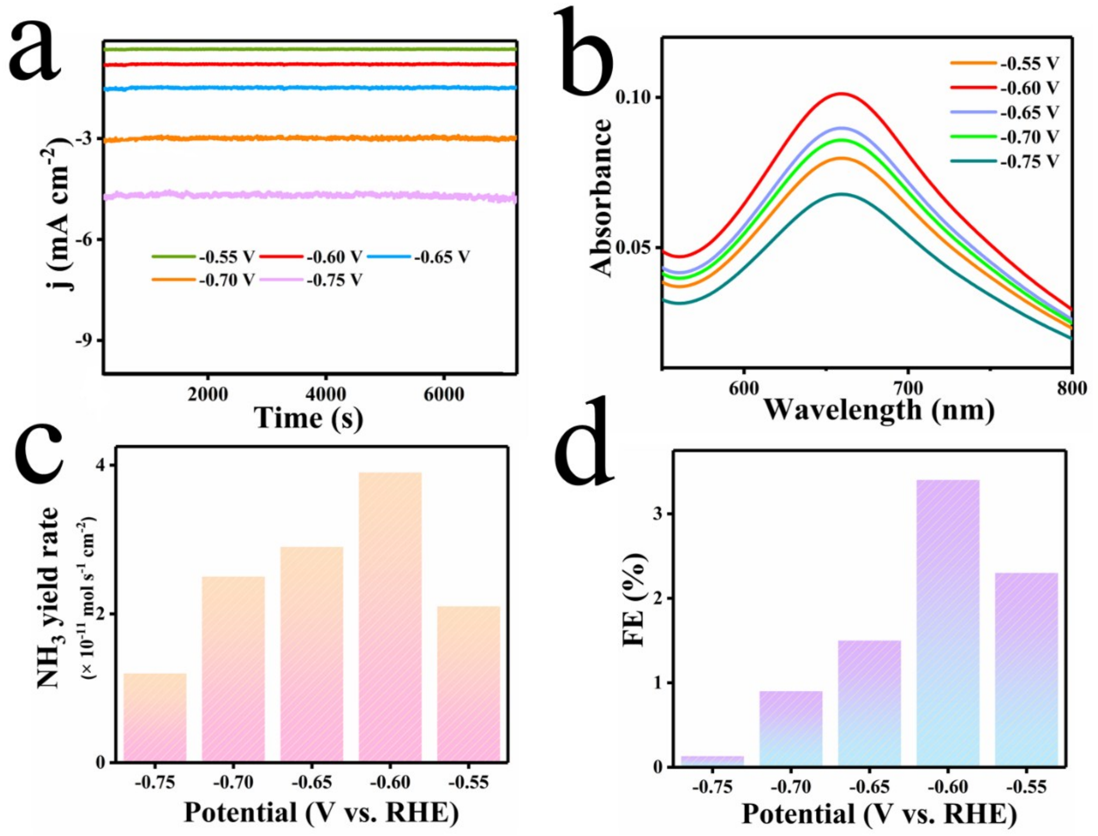

Fig. S6. (a) Time dependent current density curves at various potentials Ag/CPE in 0.05 M HCl. (b) UV-Vis absorption spectra of the electrolytes colored with indophenol indicator after 2-h NRR electrolysis at different potentials. (c) NH_3 yield rates and (d) FEs at corresponding given potentials.

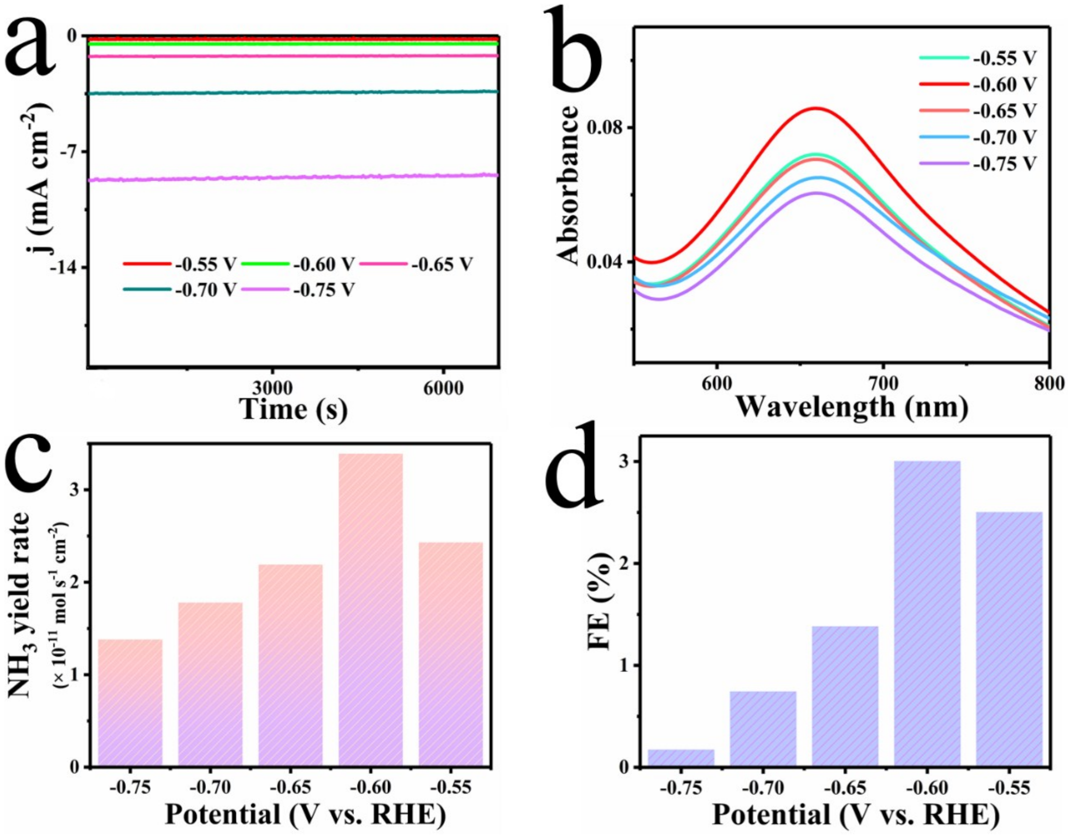

Fig. S7. (a) Time dependent current density curves at various potentials Ag/CPE in 0.2 M HCl. (b) UV-Vis absorption spectra of the electrolytes colored with indophenol indicator after 2 h NRR electrolysis at different potentials. (c) NH_3 yield rates and (d) FEs at corresponding given potentials.

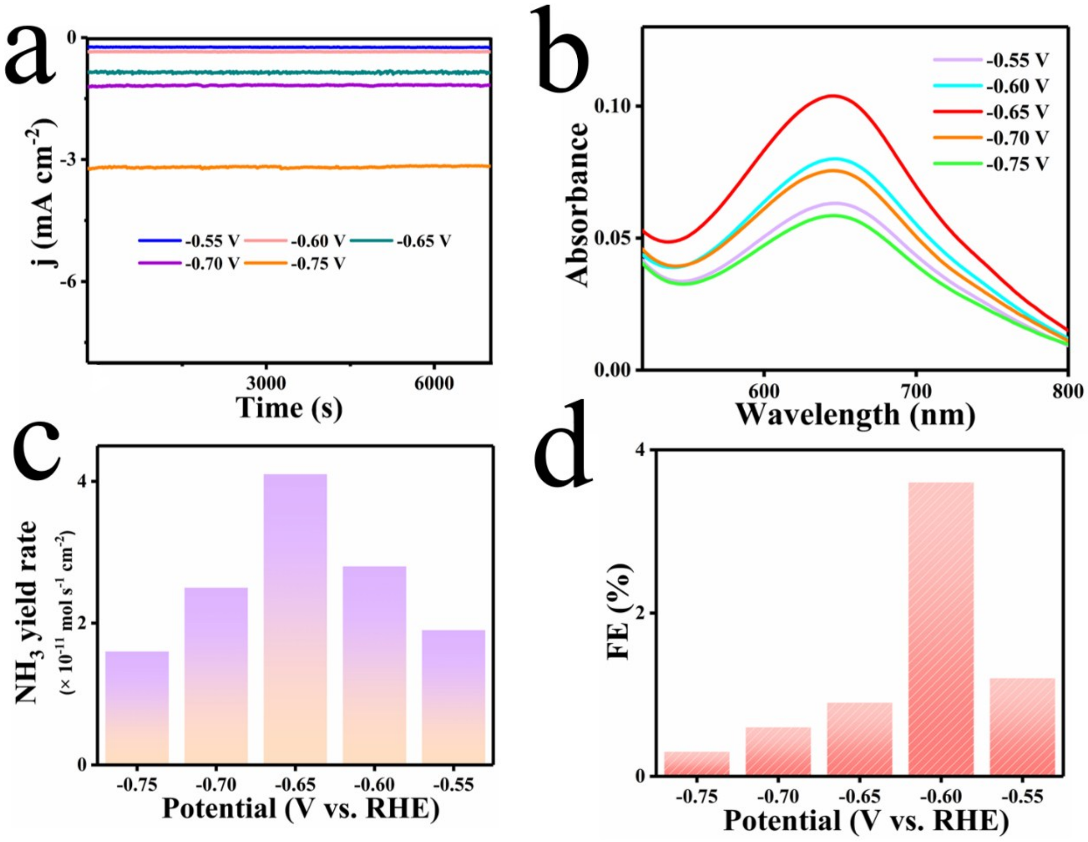

Fig. S8. (a) Time dependent current density curves at various potentials Ag/CPE in 0.5 M LiClO$_4$. (b) UV-Vis absorption spectra of the electrolytes colored with indophenol indicator after 2 h NRR electrolysis at different potentials. (c) NH$_3$ yield rates and (d) FEs at corresponding given potentials.

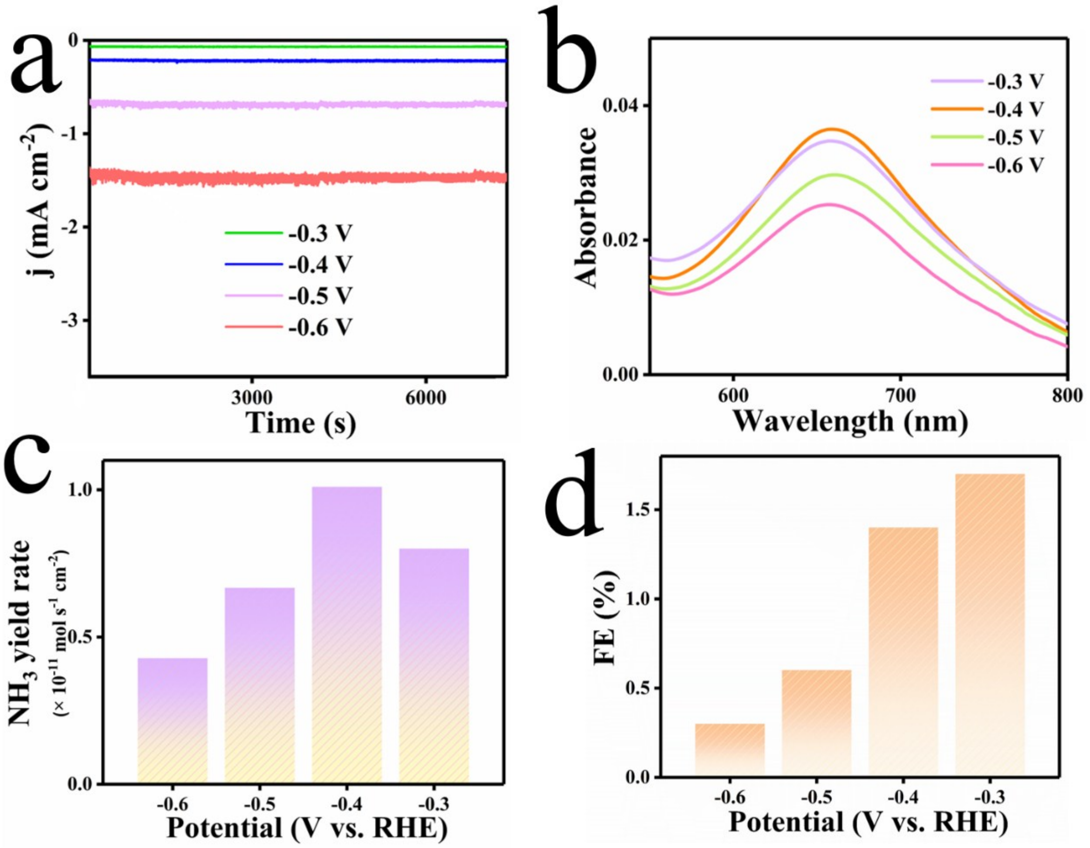

Fig. S9. (a) Time dependent current density curves at various potentials Ag/CPE in 0.1 M KOH. (b) UV-Vis absorption spectra of the electrolytes colored with indophenol indicator after 2 h NRR electrolysis at different potentials. (c) NH_3 yield rates and (d) FEs at corresponding given potentials.

Table S1. Comparison of the NRR performances for Ag/CPE with other reported NRR electrocatalysts at ambient conditions.

Catalyst	Electrolyte	Conditions	NH_3 yield rate	FE (%)	Ref.
Ag/CPE	0.1 M HCl	25 ^{o}C	4.62×10^{-11} mo1 s^{-1} cm^{-2}	4.8	This work
Mo nanofilm	0.01 M H_2SO_4	25 °C	3.09×10^{-11} mo1 s^{-1} cm^{-2}	0.72	4
PEBCD/C	0.5 M Li_2SO_4	25 °C	2.58×10^{-11} mo1 s^{-1} cm^{-2}	2.85	5
Fe_2O_3-CNT	$KHCO_3$	20 °C	0.36×10^{-11} mo1 s^{-1} cm^{-2}	0.15	6
MoS_2/CC	0.1 M Na_2SO_4	25 °C	8.08×10^{-11} mo1 s^{-1} cm^{-2}	1.17	7
MoO_3	0.1 M HCl	25 °C	29.43 μg h^{-1} mg$^{-1}_{cat.}$	1.9	8
Fe_3O_4/Ti	0.1 M Na_2SO_4	25 °C	5.6×10^{-11} mo1 s^{-1} cm^{-2}	2.6	9
Mo_2N	0.1 M HCl	25 °C	78.4 μg h^{-1} mg$^{-1}_{cat.}$	4.5	10
MoN	0.1 M HCl	25 °C	3.01×10^{-10} mo1 s^{-1} cm^{-2}	1.15	11
VN	0.1 M HCl	25 °C	8.40×10^{-11} mol s^{-1} cm^{-2}	2.25	12
Ru/C	2 M KOH	20 ^{o}C	0.34×10^{-11} mo1 s^{-1} cm^{-2}	0.28	13
a-Au/CeO_x-RGO	0.1 M HCl	25 °C	8.3 μg h^{-1} mg$^{-1}_{cat.}$	10.10	14
TiO_2	0.1 M Na_2SO_4	25 °C	9.16×10^{-11} mol s$^{-1}\cdot$cm^{-2}	2.5%	15
TiO_2-rGO	0.1 M Na_2SO_4	25 °C	15.13 μg h^{-1} mg$^{-1}_{cat.}$	3.3%	16

References

1 Z. Yi, X. Li, X. Xu, B. Luo, J. Luo, W. Wu, Y. Li and Y. Tang, *Colloid. Surface. A,* 2011, **392**, 131−136.

2 D. Zhu, L. Zhang, R. E. Ruther and R. J. Hamers, *Nat. Mater.,* 2013, **12**, 836–841.

3 G. W. Watt and J. D. Chrisp, *Anal. Chem.,* 1952, **24**, 2006–2008.

4 D. Yang, T. Chen and Z. Wang, *J. Mater. Chem. A,* 2017, **5**, 18967–18971.

5 G. Chen, X. Cao, S. Wu, X. Zeng, L. Ding, M. Zhu and H. Wang, *J. Am. Chem. Soc.,* 2017, **139**, 9771−9774.

6 S. Chen, S. Perathoner, C. Ampelli, C. Mebrahtu, D. Su and G. Centi, *Angew. Chem., Int. Ed.,* 2017, **56**, 2699–2703.

7 L. Zhang, X. Ji, X. Ren, Y. Ma, X. Shi, Z. Tian, A. M. Asiri, L. Chen, B. Tang and X. Sun, *Adv. Mater*., 2018, **30**, 1800191.

8 J. Han, X. Ji, X. Ren, G. Cui, L. Li, F. Xie, H. Wang, B. Li and X. Sun, *J. Mater. Chem. A,* 2018, **6**, 12974−12977.

9 Q. Liu, X. Zhang, B. Zhang, Y. Luo, G. Cui, F. Xie and X. Sun, *Nanoscale,* 2018, **10**, 14386–14389.

10 X. Ren, G. Cui, L. Chen, F. Xie, Q. Wei, Z. Tian and X. Sun, *Chem. Commun.,* 2018, **54**, 8474 – 8477.

11 R. Zhang, Y. Zhang, X. Ren, G. Cui, A. M. Asiri, B. Zheng and X. Sun, *ACS Sustainable Chem. Eng.*, 2018**, 6**, 9545–9549.

12 R. Zhang, Y. Zhang, X. Ren, G. Cui, A. M. Asiri, B. Zheng and X. Sun, *ACS Sustainable Chem. Eng.,* 2018, DOI: 10.1021/acssuschemeng.8b01261.

13 V. Kordali, G. Kyriacou and C. Lambrou, *Chem. Commun.,* 2000, **17**, 1673–1674.

14 S. Li, D. Bao, M. Shi, B. Wulan, J. Yan and Q. Jiang, *Adv. Mater*., 2017, **29**, 1700001.

15 R. Zhang, X. Ren, X. Shi, F. Xie, B. Zheng, X. Guo and X. Sun, *ACS Appl. Mater. Interfaces*, 2018, **10**, 28251–28255.

16 X. Zhang, Q. Liu, X. Shi, A. M. Asiri, Y. Luo, T. Li and X. Sun, *J. Mater. Chem. A*, 2018, DOI: 10.1039/C8TA05627G.